

RADIATION SIMULATIONS FOR A PRE-SEPARATOR AREA FOR RARE ISOTOPE PRODUCTION VIA PROJECTILE FRAGMENTATION*

I. Baek[#], R. M. Ronningen, Marc Hausmann, D. Lawton, A. F. Zeller, and Georg Bollen, NSCL, East Lansing, MI 48824, U.S.A.

Abstract

To support pre-conceptual research and development for rare isotope beam production via projectile fragmentation at the Rare-Isotope Accelerator facility or similar next-generation exotic beam facilities, the interactions between primary beams and beryllium and liquid-lithium production targets in the fragment pre-separator area were simulated using the Monte-Carlo radiation transport code PHITS. The purpose of this simulation is to determine the magnitude of the radiation fields in the pre-separator area so that levels of hadron flux and energy deposition can be obtained. It was of particular interest to estimate the maximum radiation doses to magnet coils and other components such as the electromagnetic pump for a liquid-lithium loop, and to estimate component lifetimes.

OVERVIEW

A key feature of working with high-intensity rare isotope beams is the capability to deliver sufficiently pure beams to the experimental setups. The level of purity needed requires the use of two stages of separation; a pre-separator and a main separator. The function of the pre-separator is to provide a well-defined location where the primary beam and most of unwanted fragments can be collected. It is shown at the left side of the Fig. 1. A pre-separator stage removes the primary beam and most of unwanted fragments. The main separator is used to further purify the beam.

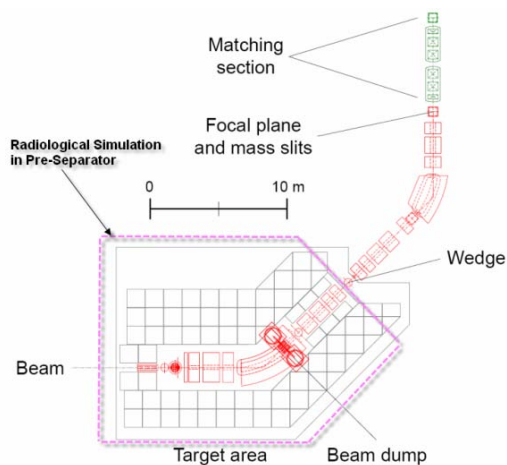


Figure 1: The schematic layout of the pre-separator. The first focus occurs directly after the first dipole, where the primary beam and unwanted fragments can be collected. The high radiation area, which is serviced by the remote-handling equipment, is indicated by the outline and the hatched area.

*Work supported by DE-FG02-04ER41313

[#]baek@nscl.msu.edu

Understanding the radiation fields in the pre-separator area is critical for the ion optical design as well as for the choice of optical components and shielding. The pre-separator will include a radiation-tolerant multipole magnet, located just behind the beam dump, and superconducting quadrupole magnets after the dipole magnet. The goal of these initial simulations was to determine the magnitude of the radiation fields in the pre-separator area. The levels of hadron flux and heating were also obtained from these calculations. It was of particular interest to estimate the maximum heating of the magnet coils and pumps and to check that the expected lifetimes are greater than one year.

OVERALL LAY OUT AND MAGNETIC FIELD SET UP

The pre-separator area includes target, nine quadrupoles, one multipole, and one dipole. First quadrupole triplets were placed between target and dipole and BNL-designed geometries were used for first three quadrupoles. A multipole and six quadrupoles were placed after the dipole and simplified cylindrical geometries were used for these magnets. Magnetic fields were implemented in the quadrupoles and the dipole. The multipole magnetic field was not included due to code limitations. One quadrupole (Q0) was placed (without magnetic field) upstream of the target module for the purpose of calculating heating. High density concrete shielding was placed before target module. Overall pre-separator layout used in Monte Carlo simulation is shown in Fig. 2.

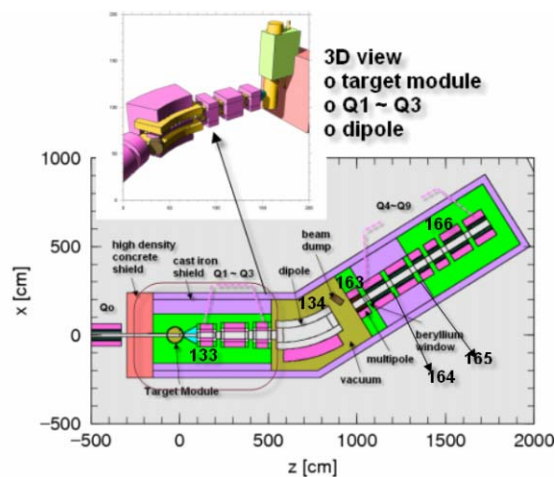


Figure 2: Overall pre-separator geometry used in Monte Carlo simulation. The numbers represent the regions for dose calculations.

The target thickness, the primary beam magnetic rigidity (B_p) after passing through the target, and fragment rigidity were determined by using the LISE++ code [1]. Since the system bend angle and dipole bend angle are different, a correction factor was applied for the magnetic field in the dipole. The optimum target thickness, the beam B_p , and the fragment B_p are given in Table 1 and Table 2. The magnetic fields of the quadrupoles are given in units of ratios (Table 3) to magnetic field of the dipole.

Table 1: Beam Properties for a Liquid Lithium Target (density = 0.507 g/cm³)

Projectile	Energy (MeV/u)	Fragment	Thickness (mg/cm ²)	$B_{p\text{frag}}/B_{p\text{beam}}$
⁴⁸ Ca	500	⁴² Si	7865	~1.33
⁴⁸ Ca	350	²² C	3300	~1.72
⁸⁶ Kr	520	⁷⁸ Ni	5300	~1.25
¹³⁶ Xe	500	¹²² Zr	3500	~1.31
²³⁸ U	400	²⁰⁰ W	1100	~1.08

Table 2: Beam Properties for a Beryllium Target (density = 1.848 g/cm³)

Projectile	Energy (MeV/u)	Fragment	Thickness (mg/cm ²)	$B_{p\text{frag}}/B_{p\text{beam}}$
⁴⁸ Ca	500	⁴² Si	8188	~1.33
⁸⁶ Kr	520	⁷⁸ Ni	5311	~1.24
¹³⁶ Xe	500	¹²² Zr	3666	~1.31

Table 3: Optical Elements for Quadrupoles and Dipole

Magnet	Radius or Half Gap (m)	Length (m)	Ratio of Magnetic Field to Magnetic Field of Dipole
Quadrupole 1	0.15	1.0	1.5
Quadrupole 2	0.20	1.5	1.5
Quadrupole 3	0.25	1.0	1.5
Dipole	0.60	5.25 (radius)	1.0
Quadrupole 4	0.25	1.25	1.5
Quadrupole 5	0.25	1.25	1.5
Quadrupole 6	0.25	0.75	1.0
Quadrupole 7	0.25	0.75	1.0
Quadrupole 8	0.25	1.25	1.5
Quadrupole 9	0.25	1.25	1.5

TRACKING PRIMARY AND SECONDARY PARTICLES

Fig. 3 shows the radioactive beams possible with a high-energy fragment separator. The colors indicate families of fragment B_p -to-beam B_p . Fig. 4 shows the

locations of the primary beams for the given families. Trajectories of all tested beams and fragments transported in the PHITS [2] simulations agreed with results from standard ion-optics calculations. The physical location of primary beam, ⁴⁸Ca having 500 MeV/u, at the beam dump as tracked in the simulation is shown in Fig. 5. The desired fragment ⁴²Si passes through system as expected and this is shown in Fig. 6.

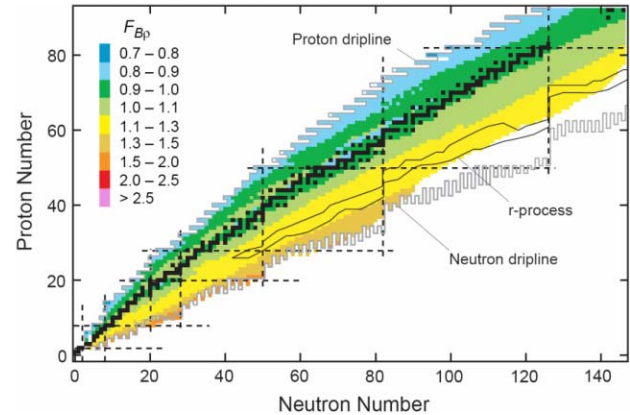


Figure 3: The ratio $F = B_p(\text{fragment})/B_p(\text{beam})$ of the magnetic rigidity of a given fragment to that of the primary beam. The location of the primary beam at the position of the beam dump for the different values of F is shown in Fig. 4 with the same color code.

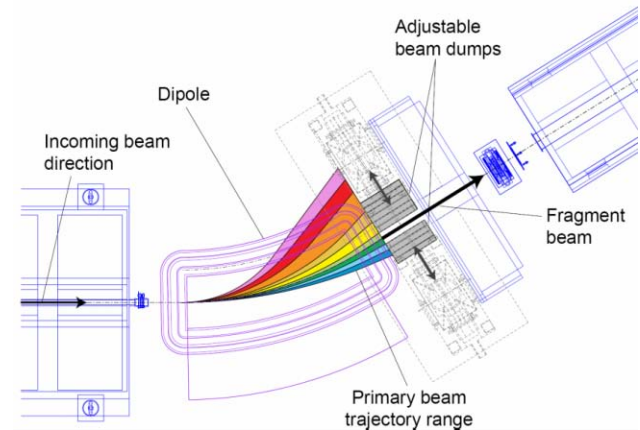


Figure 4: Separation of primary beams from the selected fragment beam as a function of F using the color code given in Fig. 3.

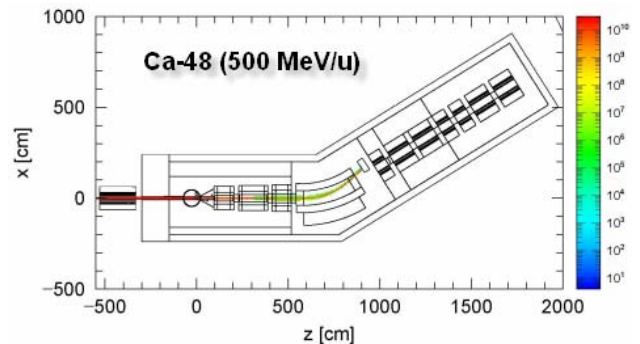


Figure 5: ⁴⁸Ca (500 MeV/u) with liquid lithium target.

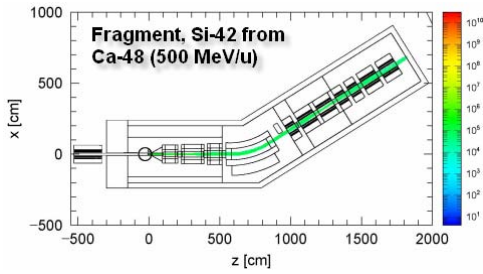


Figure 6: ^{42}Si from ^{48}Ca (500 MeV/u) with liquid lithium target.

PROMPT DOSE RATES IN AIR INSIDE SHIELDING

The particle fluxes and the radiation dose rates from neutrons and photons in the air inside pre-separator area shielding during operations were studied using the ^{48}Ca beam with 500 MeV per nucleon at 400 kW by simulations using the PHITS code system. The purpose of calculating fluxes and radiation dose rates inside shielding is to estimate optimum shielding thickness necessary to reduce the radiation dose rates outside of shielding below regulatory limits. It was determined that the ^{48}Ca beam produces one of the highest dose rates expected of beams to be delivered to the fragmentation target area. Therefore, the ^{48}Ca beam was chosen for this study. The beam line and air regions are shown in Fig. 2.

Table 4: shows the dose equivalent rates in specified regions from neutrons and photons.

Table 4: Dose Equivalent Rates

Region	Dose Rates (mrem / hr)	
	Neutron	Photon
133	1.78E+14	1.34E+12
163	7.38E+09	4.94E+07
164	4.87E+08	5.45E+06
165	1.78E+08	1.65E+06
166	3.04E+07	2.25E+05
167	7.08E+06	6.85E+04

HEATING CALCULATION, DAMAGE, AND LIFE TIME OF SUPERCONDUCTING COILS

The heat in the superconducting coils was calculated using PHITS code system. The unit of heat from PHITS outputs is MeV/cm^3 . Fig. 7 shows a representative example of the heating distribution in the pre-separator area from PHITS simulations.

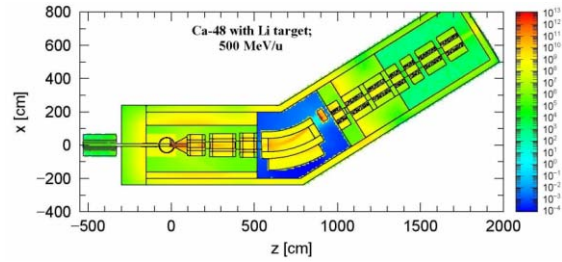


Figure 7: Heating in the pre-separator area for the 400 kW ^{48}Ca beam and the liquid lithium target. (unit : MeV/cm^3).

The Table 5 shows the maximum energy depositions in coils for the tested projectiles, where the specific power deposition (mW/cm^3) is given in units of dose rate (Gy/yr). It is likely that the pre-separator will operate about 1/3 of each year. Data on the radiation sensitivity of BNL HT superconducting material is not available. To get approximate values, the radiation sensitivity of Nb_3Sn (500 mGy) was used to calculate the life times of coils of the quadrupoles in pre-separator area (Table 6.)

Table 5: Dose Rates in Coils for the Tested Projectiles (Unit: Gy/yr)

Target	Liquid Lithium	Beryllium		
		^{48}Ca	^{86}Kr	^{136}Xe
Projectiles	^{238}U	^{48}Ca	^{86}Kr	^{136}Xe
Energy (MeV)	400	500	520	500
Q1	1.51E+07	6.43E+07	2.90E+07	1.70E+07
Q2	3.78E+06	1.51E+07	7.57E+06	4.42E+06
Q3	2.52E+06	9.46E+06	2.52E+06	1.89E+06

Table 6: The Life Times of Coils for the Tested Beams (Unit: year)

Target	Liquid Lithium	Beryllium		
		^{48}Ca	^{86}Kr	^{136}Xe
Projectiles	^{238}U	^{48}Ca	^{86}Kr	^{136}Xe
Energy (MeV)	400	500	520	500
Q1	3.30E+01	7.77E+00	1.72E+01	2.94E+01
Q2	1.32E+02	3.30E+01	6.61E+01	1.13E+02
Q3	1.98E+02	5.28E+01	1.98E+02	2.64E+02

CONCLUSION

The trajectories of beams and fragments when transported in the PHITS simulations agree with results from standard ion-optics calculations. Neutron and proton fluxes in air inside shielding have been calculated. Maximum heating, the energy deposition, and the estimation of life time on coil have been calculated from PHITS simulation.

REFERENCES

- [1] <http://dnr080.jinr.ru/lise/lise.html>. (2006)
- [2] H. Iwase, K. Nitta and T. Nakamura, J. Nucl. Sci. Technol. 39 (2002) 1142.